

# Dynamic phase transition in the conversion of B-DNA to Z-DNA

Jaya Maji\* and Somendra M. Bhattacharjee†

*Institute of Physics, Bhubaneswar-751005, India*

(Dated: September 1, 2018)

The long time dynamics of the conformational transition from B-DNA to Z-DNA is shown to undergo a dynamic phase transition. We obtained the dynamic phase diagram for the stability of the front separating B and Z. The instability in this front results in two split fronts moving with different velocities. Hence, depending on the system parameters a denatured state may develop dynamically even though it is thermodynamically forbidden. This resolves the current controversies on the transition mechanism of the B-DNA to Z-DNA.

## I. INTRODUCTION

The most common form of DNA found under normal physiological low salt conditions is the B-DNA, the well known double helix with a right handed helicity. Quite surprisingly, the first DNA structure to be solved by X-ray crystallography turned out to be a left handed zig-zag form called the Z-DNA[1–3]. This Z-DNA can be stabilized in vitro in presence of high salt concentration, cations or negative super-coiling. Although the Z form is transient in vivo due to the lack of friendly environment, still the B-Z conversion is relevant in poxviruses[4], and Alzheimer’s disease[5]. Apart from the inversion of helicity, the Z-DNA has a repeat unit of 2 base pairs compared to one for B. Thus a conformational transformation from the B to the Z form takes place as, e.g., the ionic concentration or super-coiling is changed. The B-Z transition is first order in nature[1, 6–9].

As the base pairs and a subset of backbone sugar rings have to flip to execute the B-Z transition involving changes in helical chirality, the dynamics offers intriguing possibilities[2]. Only recently methods have been developed to explore the dynamics in single DNA as opposed to earlier studies in solutions, though with conflicting results. In Ref. [10] the B-Z conformational transformation for a short 15 base pair GT (non-Watson-Crick wobble base pair) DNA wrapped on a single walled carbon nanotube was monitored as a function of time by the addition of counter-ions. The nanotube helped in identifying the phases via accurate measurements of the band-gap in a simpler geometry. This transition is completely reversible and is thermodynamically identical to the transition seen in the absence of the nanotube. *The results seem to indicate the formation of a denatured DNA during the transformation, even though a denatured state under the experimental conditions is not possible thermodynamically.* A different single molecule experiment studied the transition under a tension and negative super-helicity by combining FRET with magnetic tweezers[11]. This experiment on an effectively  $(GC)_{11}$  DNA (i.e. 22 bases) *seems to favour a single interface between B and Z with-*

*out any denatured bubble.*

One can characterize the B-Z transformation by a growth of a suitable domain over the bulk of DNA. In any such scenario, the B-Z interface, the separator between the two chiral phases, plays an important role. The equilibrium interface has been characterized structurally and from other studies. The structure of a short oligomer in presence of a Z-DNA binding protein at 2.6Å resolution indicates broken base pairs separating the B and the Z phases. The protein acting as an external source inducing the transition is expected to produce a sharp interface[12]. A very ingenious way of studying the interface is to use mirror DNA[13, 14], though it cannot be used for chirality changing transition. Interfacial studies and melting of short B-B\* oligomers, where B\* is the enantiomer of B, show that the junction mimics the B-Z junction, and the interface broadens as the melting point is reached. In contrast to these equilibrium cases, the nature of the interface during the transition depends on the nature of the transition mechanism[7, 8]. Several such schemes are in vogue and discussed in detail in Ref. [2]. The two main competing hypothesis for the B to Z transition mechanism are the following. It is either via (1) the base pair separation followed by base pair flipping[1], or (2) the base pair flipping without any base pair separation[6]. In the first case there could be a denatured intermediate state while in the second there could be a Z type but following the standard Watson-Crick base pairing (ZWC-DNA).

The apparently contradictory results from the two single molecule experiments and the controversy associated with the B-Z transition mechanism in general, motivate us to study a coarse-grained thermodynamic model for the dynamics. This implicitly requires infinitely long chains, since small length DNAs or oligo-nucleotides do not show any proper thermodynamic phase transition. Inducing the B to Z transition is tantamount to a lowering of the free energy of Z compared to B making Z the most preferable state. We in our formulation use the simplification of the single molecule experiments to restrict the geometry to one-dimension only. The boundaries of the long chain are maintained in the two states so that the new structure develops from one side. In such a problem the dynamics of the transition produces a steady state with uniformly moving front (or fronts). An investigation of the various types of fronts would help us answer

---

\*Electronic address: jayamaji@iopb.res.in

†Electronic address: somen@iopb.res.in

the question of any dynamic generation of thermodynamically forbidden state.

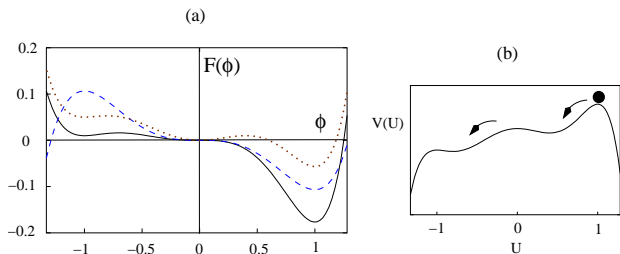


FIG. 1: (a) The Landau function  $F(\phi)$  as a function of  $\phi$ . In all cases,  $\phi = 1$  is the stable state, Z-DNA,  $\phi = -1$  represents an unstable (dashed line) or metastable (solid and dotted lines) state, B-DNA while  $\phi = 0$  is a quadratically unstable (solid and dashed lines) or metastable (dotted line) state, denatured state. The three cases I, II and III in the text correspond to dotted, solid and dashed lines. (b) Potential  $V(U) = -F(U)$  for the particle-on-a-hill analogy.

## II. MODEL

Our model consists of three states B, the denatured state and Z to be represented by a parameter  $\phi = -1, 0, 1$ . The space time coordinates  $z, t$  are taken to be continuous. It is a one dimensional problem where  $\phi(z, t)$  describes the state of the coarse-grained base-pair at index  $z$  along the DNA. For the B-Z transition, we take  $\phi = -1$  (B state) to be unstable (or metastable) which is getting invaded by the stable state at  $\phi = 1$  (Z state). We study this phenomenon through a Landau free energy  $F(\phi)$  taken as a sixth order polynomial with the coefficients chosen to have extrema at  $\phi = 0, \pm 1$ . This is ensured by choosing the thermodynamic force  $f(\phi)$  as

$$f(\phi) = -\frac{dF(\phi)}{d\phi} = \phi(\phi + \alpha)(\phi - \beta)(1 - \phi)(1 + \phi), \quad (1)$$

where  $\alpha, \beta > 0$  are constants, whose values are system specific. Needless to say, the relative stability of the three phases can be adjusted by  $\alpha, \beta$ . The Landau Ginzburg free energy is taken as

$$\mathcal{H}(\phi) = \int dz \left[ \frac{D}{2} \left( \frac{\partial \phi}{\partial z} \right)^2 + F(\phi) \right], \quad (2)$$

where  $D > 0$  is the elastic constant.  $D$ -term allows inhomogeneity, e.g., at the interface between two phases. The three homogeneous phases are given by the minima of the Landau free energy  $F(\phi)$ . The dynamics is governed by the non linear diffusion equation

$$\frac{\partial \phi}{\partial t} = D \frac{\partial^2 \phi}{\partial z^2} + f(\phi), \quad (3)$$

derived from Eq. 2 in the overdamped limit. The friction coefficient has been absorbed in the definition of time  $t$ .

The geometry to be considered is such that the B state is on one side and the Z state on the other with the front moving towards the unstable state. For the B-Z case, this is ensured by the boundary conditions

$$\phi(z \rightarrow -\infty) = 1, \quad \phi(z \rightarrow \infty) = -1$$

for Eq. 3 for all time. A few other boundary conditions are considered too. The three generic cases obtained by fixing  $\alpha$  and  $\beta$  are the following (see Fig. 1a)

- Case I : While quenching to the stable state, Z, state B remains in a metastable state while the denatured state  $\phi = 0$  is also metastable. Since the barriers are somewhere in between  $\phi = -1$  and  $\phi = 1$ , we have  $0 \leq \alpha, \beta < 1$ .
- Case II : The metastable state (B-DNA) sees a barrier somewhere in between  $-1$  to  $0$ , while the denatured state is quadratically unstable state. This case is for  $0 < \alpha < 1$ , and  $\beta = 0$ .
- Case III : Unstable B state quenched into stable Z while the denatured state remains in a quadratically unstable state (i.e., without facing any barrier). This happens when  $\alpha > 1$  and  $\beta = 0$ .

To be noted that cases I and II are similar to the free energy landscape obtained in Ref. [15] as the potential of the mean force obtained from molecular dynamics.

The diffusive like term in Eq. 3 coming from the elastic part of Eq. 2 tends to smoothen out any inhomogeneity while the driving force  $f(\phi)$  tends to favour the stable state whenever there is any inhomogeneity. The combined effect of the diffusion like spreading and the selection of one phase by the drive leads to a steady state where the interface shows a uniform motion and takes a shape which is not necessarily the equilibrium shape [16]. Based on the Fisher-Kolmogorov (F-K) idea, the traveling wave solution  $\phi(z, t) = U(z - vt)$  can be used to rewrite Eq. 3 as

$$\frac{d^2 U}{d\tau^2} + v \frac{dU}{d\tau} + f(U) = 0, \quad (\tau = z - vt), \quad (4)$$

where  $v$  the velocity of the front is to be determined. The interface which we are studying is between  $\phi = +1$  and  $\phi = -1$  states. Eq. 4 can be interpreted as the motion of a particle moving in a potential  $V = -F(U)$  (Fig. 1b) starting at the hill at  $U = +1$  at time  $\tau = -\infty$  just reaching the other hill at  $U = -1$  at time  $\tau = +\infty$  losing energy due to “friction”  $v$ . For a given potential, such a motion is possible only for particular values of  $v$  and that velocity is the selected velocity of the front. However, it is also possible that the particle spends an infinite amount of time in the intermediate state so that the descent from  $U = +1$  to  $U = 0$  and the descent from  $U = 0$  to  $U = -1$  are independent requiring two different friction coefficients. The physical picture that emerges is that the stable state moves towards the unstable state, and the propagating front will have a time

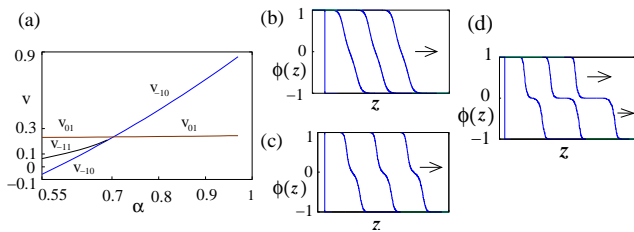


FIG. 2: (a) Plot of velocity  $v$  vs  $\alpha$  for a fixed value of  $\beta = 0.45$ . Three velocities meet at a common point at  $\alpha_c(\beta)$ . The remaining three figures ( $\phi$  vs  $z$ ) represent the time evolution of the front (or fronts). (b) A single front for  $\alpha = 0.6 < \alpha_c(\beta)$ . (c) A single front for  $\alpha = 0.7$  near  $\alpha_c(\beta)$  with a signature of the width widening but no “0” phase. (d) For  $\alpha = 0.72 > \alpha_c(\beta)$  single front splits into two fronts.

independent shape and a constant velocity  $v$ . However in some situations, the initial big front separating the two phases  $\phi = \pm 1$  splits into two, one front between  $\phi = -1$  and  $\phi = 0$ , while the other one between  $\phi = 0$  and  $\phi = 1$ . The two smaller fronts move with different shapes and speeds  $v_{-10}, v_{01}$ . The  $\phi = 0$  state may then get dynamically generated. Consequently one may see the development of the denatured state. The less preferable state will eventually be devoured by the stable state completing the transition from B to Z-DNA.

### III. DYNAMIC PHASE DIAGRAM-NUMERICAL AND PERTURBATIVE APPROACH

The velocity of the front has been determined by numerical analysis for different boundary conditions like (a)  $\phi(-\infty, t) = 1, \phi(\infty, t) = -1$  for the B-Z front, (b)  $\phi(-\infty, t) = 1, \phi(\infty, t) = 0$  for a front between Z and the denatured state, (c)  $\phi(-\infty, t) = 0, \phi(\infty, t) = -1$  for a front between B and the denatured state. The initial ( $t = 0$ ) interface of width  $w$  is located at  $z = z_0$  and a Crank Nicolson method is used to evolve the nonlinear diffusion equation. Once a steady state is reached, the velocity is determined by locating the positions at which  $\phi = \pm 0.5$ , and  $\phi = 0$  as appropriate. In the case of the split front, only the velocity  $v_{01}$  can be obtained by the F-K analysis but not in general.

The dependence of the velocities on  $\alpha$  for a fixed  $\beta$  is shown in Fig. 2a. We see that three fronts move with different velocities for  $\alpha < \alpha_c(\beta)$  with  $v_{01} > v_{-11} > v_{-10}$ . All these velocities are same at  $\alpha = \alpha_c(\beta)$ . For  $\alpha > \alpha_c(\beta)$ , the BZ front splits into two fronts and the denatured state grows with time as  $(v_{-10} - v_{01})t$ . It is straightforward to see that no stable front between  $\pm 1$  can exist if  $v_{-10} < v_{01}$ . Also the  $v_{-11}$  curve ends at  $\alpha_c(\beta)$  and has no continuation for  $\alpha > \alpha_c(\beta)$ . This indicates that  $\alpha_c(\beta)$  is a singular point. The numerically determined  $\alpha_c(\beta)$  vs  $\beta$  line is shown in Fig. 3. This is the *phase diagram for dynamics* with the phase boundary as

the limit of stability of the BZ front (from below).

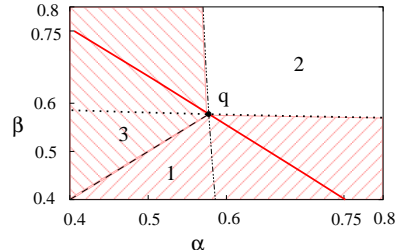


FIG. 3: Dynamic phases in a plot of  $\alpha$  vs  $\beta$ , the boundary (solid line) being given by  $\alpha = \alpha_c(\beta)$ . In the region below the boundary line, a single front between  $-1$  to  $1$  (big front) propagates without splitting. In the region above the boundary line the front between  $-1$  to  $+1$  splits into two (small) fronts. Z, “0” and B are the stable states in regions 1, 2 and 3 respectively. The dotted line corresponds to  $v_{01} = 0$ , while the dash-dotted line to  $v_{-10} = 0$ . The split fronts move away from each other in region 2, both towards right in 1 and both towards left in 3, as per the chosen boundary conditions. The big front has zero velocity on the  $\alpha = \beta$  line and the diagram is symmetric around this line. Point q represents the equilibrium point, where three states have the same free energy.

The phase diagram can be confirmed by considering a few special cases. For  $\alpha = \beta$ , the free energies of B and Z are same and the BZ front should have zero velocity. The point  $\alpha = \beta = \frac{1}{\sqrt{3}}$  corresponds to the equilibrium situation, for which all the three fronts are static, and therefore the condition to be on the phase boundary is trivially satisfied. This point is denoted by q in Fig. 3. Along the  $\alpha = \beta$  line for  $\alpha < \alpha_c(\beta)$ ,  $v_{01}, v_{-10} \neq 0$  with state  $+1$  or  $-1$  invading 0. In contrast in region 2, along the same  $\alpha = \beta$  line, “0” is the stable state and it invades both  $\pm 1$  states. In region 2 above the dotted line, obtained by equating  $F(1) = F(0)$  (Eq. (1)), the “0” state grows with the two fronts moving away from each other, but below that dotted line in region 1 the Z state grows though the fronts move in the same direction (towards right). The  $Z \leftrightarrow B$  symmetry in our choice of the free energy mandates a symmetric phase diagram across the  $\alpha = \beta$  line with the fronts moving towards left in region 3.

For  $\alpha, \beta$  close to  $\alpha = \beta = \frac{1}{\sqrt{3}}$ , a perturbative analysis [17] can be done to determine the velocity, which is now a small parameter. By writing, to first order in  $v$ ,

$$U(z - vt) \approx U_0(z) + v t U'_0(z) \quad (5)$$

where prime denotes a derivative,  $v$  can be determined to first order in free energy difference if  $U_0$  is known. In the equilibrium situation, there is a Goldstone like zero-energy mode, because, the interface can be placed anywhere or shifted along  $z$  without any cost of energy. We therefore take  $U_0(z)$  as centered around an arbitrarily chosen origin. The static solution satisfies,

$$\frac{1}{2} (U'_0(z))^2 = F(U_0) = U_0^2 (U_0^2 - 1)^2. \quad (6)$$

With a first order correction, the velocities are

$$v_{ij} = \frac{\epsilon_{ij}}{\int_{-\infty}^{\infty} [U'_0(z)]^2 dz}, \quad (7)$$

where  $i, j = 0, \pm 1$ , and the free energy differences  $\epsilon_{ij}$  are

$$\epsilon_{01} = -\frac{1}{12} - 2\frac{(\alpha - \beta)}{15} + \frac{\alpha\beta}{4}, \quad (8)$$

$$\epsilon_{-10} = \frac{1}{12} - 2\frac{(\alpha - \beta)}{15} - \frac{\alpha\beta}{4}, \quad (9)$$

$$\epsilon_{-11} = -4\frac{(\alpha - \beta)}{15}. \quad (10)$$

At this perturbative regime, by equating the velocities, we find that around  $\alpha = \beta = \frac{1}{\sqrt{3}}$ , the slope of the critical line is  $-1$ , which is consistent with the numerically determined boundary shown in Fig. 3. Moreover we also find the phase boundary to deviate very slightly from a straight line over the range shown there. There is a deviation from linearity beyond that but the numerical error becomes larger. We next study the behavior of the width

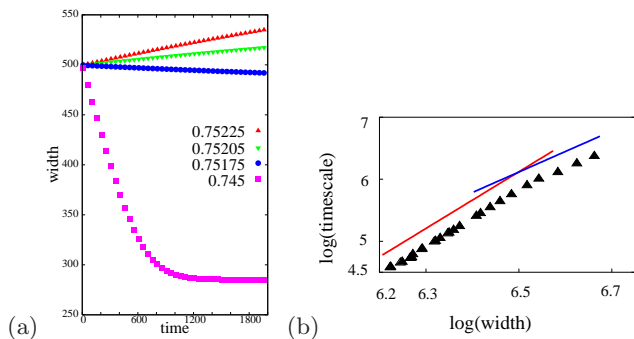


FIG. 4: (a) Time evolutions of the width (in arbitrary units) of the front are shown for different values of  $\alpha$  keeping  $\beta = 0.4$  fixed. The initial front had a stretch of “0” phase which decays for  $\alpha < \alpha_c(\beta)$  but grows linearly for  $\alpha > \alpha_c(\beta)$ . The timescale to reach saturation increases as  $\alpha \rightarrow \alpha_c(\beta)^-$ . For this case  $\alpha_c(\beta) \approx 0.752$ . (b) Log-Log plot of width versus time scale for  $\alpha < \alpha_c(\beta)$ . Two solid line slopes are shown far from and near  $\alpha_c(\beta)$ .

of the interface and of the appropriate timescale for the dynamics. For the special case of  $\beta = 0.5$  as  $\alpha \rightarrow \alpha_c(\beta)$  the divergence of the width has been noted in Ref. [18]. At  $\alpha = \beta = \frac{1}{\sqrt{3}}$ , any length of “0” domain can be inserted and therefore the width of the BZ interface at the limit of stability is infinity. On the split-front side (Fig. 2d), the width increases linearly with time as  $W = (v_{01} - v_{-1,0})t$  (Fig. 4a for  $\alpha = 0.75205$ ). While, on the other side of the phase boundary the single front (Fig. 2b) has a finite width (Fig. 4a for  $\alpha = 0.745$ ). Close to the phase boundary though a deformation of the moving front is visible around  $\phi = 0$  (Fig. 2c), but width saturates at large time (Fig. 4a for  $\alpha = 0.75175$ ) without any appearance of the denatured phase. Hence scaling forms are expected as

$$W \sim |\alpha - \alpha_c(\beta)|^{-\mu}, \quad \tau \sim W^z.$$

Fig. 4a shows the time evolution of the width of an interface for various  $\alpha$  at a fixed  $\beta$ , where the instantaneous width  $W$  of the interface at time  $t$  is obtained as

$$W^2 = \langle z^2 \rangle - \langle z \rangle^2, \quad \text{where} \quad (11)$$

$$\langle z^n \rangle = \frac{\int z^n \left( \frac{d\phi(z,t)}{dz} \right)^2 dz}{\int \left( \frac{d\phi(z,t)}{dz} \right)^2 dz}. \quad (12)$$

Another way to characterize the width would be to look at the slope of the profile *i.e.*  $\left. \frac{d\phi(z)}{dz} \right|_{\phi=0}$ , which is related to the inverse of  $W$  and also shows the scaling with characteristic dynamic exponent. We started with an interface that has an insertion of the “0” state and the width monitors the decay or the growth of the “0” state. The width saturates exponentially for  $\alpha < \alpha_c(\beta)$  albeit slowly near  $\alpha \rightarrow \alpha_c^-$ , while a linear growth is observed for  $\alpha > \alpha_c(\beta)$ . Time here refers to the discretized time in the Crank-Nicolson approach. By fitting an exponential to the time evolution of  $W$ , the characteristic time scale was determined, for  $\alpha < \alpha_c(\beta)$ . The exponent  $\mu$  is found to be rather small, not inconsistent with the logarithmic growth observed in Ref. [18]. Fig. 4b shows the log-log plot of  $\tau$  vs  $W$  indicating a value of  $z$  within 3.0 to 4.0. However for better accuracy one requires a large system and long time observation as well. The divergences of  $W$  and  $\tau$  with scaling establish the critical nature of the  $\alpha = \alpha_c(\beta)$  line.

Despite the immense success in probing the various phases of DNA by single molecular manipulation techniques, interfaces have not been explored thoroughly. We hope our results will motivate direct studies of interfaces of DNA, especially their stability. Even on the theoretical front, it remains to be seen if all atom molecular dynamics simulations that have been successful [15, 19, 20] in seeing various phases, can be used to monitor the dynamics of interfaces, B-Z in particular, under given boundary conditions.

#### IV. CONCLUSION

The conformational transition from B-DNA to Z-DNA has been studied via wave-front propagation. The dynamic phase diagram for the steady state is obtained in the  $\alpha$ - $\beta$  plane, where  $\alpha, \beta$  characterize the relative stability of the phases, by the critical value  $\alpha_c$  for different values of  $\beta$ . The phase boundary in the  $\alpha$ - $\beta$  plane has been determined and corroborated by a perturbation analysis. The dynamic transition is associated with diverging length and time scales and has its own dynamic exponent. On one side of the phase boundary the dynamics involves propagation of one B-Z interface with a uniform speed, while on the other phase such an interface is unstable leading to the formation of the thermodynamically forbidden denatured state. This in turn, suggests that there is no unique mechanism for the B-Z dynamics

and it is possible to switch from one type to other by tuning the parameters. A resolution of the controversy

in experiments is that the two cases, namely nanotube and magnetic tweezers are on the two sides of the phase boundary.

- 
- [1] Wang A. H. *et al.*, Nature London, **282**, 680 (1979).  
 [2] M. A. Fuertes *et al.*, Chem. Rev., **106**, 2045 (2006).  
 [3] See, e.g., R. Sinden R. Richard, *DNA Structure and Function*, 1994 (Academic Press, Sandiego).  
 [4] Rich A. and Zhang S., Nature Rev. Genet., **4**, 566 (2003).  
 Gagna C. E. and Lambert W. C., Med. Hypothesis, **60**, 418 (2003).  
 [5] Anitha S. *et al.*, Neuromol. Med., **2**, 289 (2002)  
 [6] Harvey S. C., Nucleic Acids Res., **11**, 4867 (1983).  
 [7] Lim W. and Feng Y. P., Biophys. J, **88**, 1593 (2005).  
 [8] Kastenholz M., Schwartz T. U. and Hüenberger P. H., Biophys. J, **91**, 2976 (2006).  
 [9] Ivanov V. I., Krylov D. Iu. and Miniati E. E., Mol. Biol. (Mosk), **19**, 390 (1985).  
 [10] Heller D. A. *et al.*, Science, **311**, 508 (2006).  
 [11] Lee M., Kim S. Ho and Hong Seok-Cheol, Proc. Natl. Acad. Sci., **107**, 4985 (2010).  
 [12] Ha S. C. *et al.*, Nature, **437**, 1183 (2005).  
 [13] Urata H. *et al.*, Biochem. Biophys. Res. Comm., **309**, 79 (2003).  
 [14] Vichier-Guerre S. *et al.*, Tetrahedron Letters, **38**, 93 (1997).  
 [15] Lee J. *et al.*, J. Phys. Chem. B, **114**, 9872 (2010).  
 [16] Murray J. D. *Mathematical Biology: An Introduction* 3rd edn(2002) (New York: Springer).  
 [17] See, e.g., Bhattacharjee S. M., J. Phys. Condens. Matter, **22**, 155102 (2010).  
 [18] Bechhoefer J., Löwen H., Tuckerman L. S., Phys. Rev. Lett., **67**, 10 (1991).  
 [19] Wereszczynski J. and Andricioaei I., PNAS, **103**(44), 16200-16205 (2006).  
 [20] Luan B. and Aksimentiev A., PRL, **101**, 118101 (2008).